J-10

An Improved Puff Algorithm for Plume Dispersion Simulation

PAOLO ZANNETTI
AeroVironment Inc., Pasadena, CA 91107

Reprinted from JOURNAL OF APPLIED METEOROLOGY, Vol. 20, No. 10, October 1981
American Meteorological Society
Printed in U. S. A.

Reprinted from JOURNAL OF APPLIED METEOROLOGY, Vol. 20, No. 10, October 1981
American Meteorological Society
Printed in U. S. A.

An Improved Puff Algorithm for Plume Dispersion Simulation

PAOLO ZANNETTI

AeroVironment Inc., Pasadena, CA 91107

(Manuscript received 26 January 1981, in final form 10 June 1981)

ABSTRACT

Recent developments in puff methods for simulating plume behavior are discussed. Modifications to the basic methodologies are introduced which make it more generally applicable to non-stationary and non-homogeneous conditions, as well as calm wind situations. The modifications described should also allow significant reductions of computer storage and running time requirements. The algorithm presented could easily be extended to the treatment of segment or area sources. The model accurately reproduces the analytical solution to the steady-state Gaussian plume equation.

1. Introduction

It is well known that the basic Gaussian approach in air pollution modeling gives a plume formula whose validity requires the main assumptions of (i) spatial homogeneity, (ii) stationary conditions and (iii) flat terrain. The basic steady-state Gaussian plume formula can be written in the following way (without ground or inversion layer reflections and without decay terms):

$$\chi = \frac{Q}{2\pi\sigma_h\sigma_z|\mathbf{u}|}\exp\left[-\frac{1}{2}\left(\frac{c}{\sigma_h}\right)^2\right] \times \exp\left[-\frac{1}{2}\left(\frac{z_s + \Delta h - z_r}{\sigma_z}\right)^2\right], \quad (1)$$

where $\chi = \chi(\mathbf{s}, \mathbf{r})$ is the concentration in $\mathbf{r} = (x_r, y_r, z_r)$ due to the emission in $\mathbf{s} = (x_s, y_s, z_s)$, Q is the emission rate, $\sigma_h = \sigma_h(j_h, d)$ and $\sigma_z = \sigma_z(j_z, d)$ are the plume standard deviations (horizontal and vertical) expressed as a function of horizontal and vertical turbulence states, j_h and j_z, and downwind distance $d = [(\mathbf{r} - \mathbf{s})\cdot\mathbf{u}]/|\mathbf{u}|$; $\mathbf{u} = (u_x, u_y, u_z)$ is the wind velocity vector; c is the crosswind distance $c = (|\mathbf{r} - \mathbf{s}|^2 - d^2)^{1/2}$; and $H = z_s + \Delta h$ is the effective emission height due to the release height z_s and the plume rise Δh. Eq. (1) is applied for $d > 0$; if $d \leq 0$, then the concentration χ is zero.

As can be easily seen, Eq. (1) refers to a stationary state (χ does not depend on time), uses meteorological conditions (wind and turbulence states) that must be considered homogeneous and stationary in the modeled area, and cannot work in calm conditions where $|\mathbf{u}| \to 0$. However, the simplicity of the Gaussian approach, its relatively easy use with clearly measurable meteorological parameters and, especially, the elevation of this methodology to the quantitative decision-controlling level (U.S. EPA, 1978), have stimulated research aimed at removing the limitations of the Gaussian theory to treat the complex situations of the real world.

One area of particular emphasis has been the identification, for complex meteorological or terrain situations, of those parameters that allow Eq. (1) to give the maximum concentration at a receptor. Other applications have used Eq. (1) in a "climatological" way to give long-term averages (monthly, seasonally, or annually) in the receptors (e.g., Martin, 1971; Runca *et al.*, 1976). In these applications, each concentration computed by Eq. (1) is weighted by the frequency of occurrence of its corresponding meteorological condition. Yet, other applications have even tried to remove the physical meaning of the parameters in Eq. (1). For example, Melli and Runca (1979) allowed the "wind speed" $|\mathbf{u}|$ to change its value as a function of d, the downwind distance, to produce ground level concentration values more similar to those obtained by finite-difference simulations in the same conditions.

In the past, the more complex time-varying applications of simulation modeling have made extensive use of dynamic grid model techniques (mainly, finite-difference simulations following the K-theory approach). However, especially recently, a growing concern has arisen about some important limitations of such a numerical approach. Specifically, 1) numerical treatment of the advection terms often produces an unreasonable, artificial diffusion, and 2) K-theory simulation of the growth of a plume from a point source is often fundamentally wrong in turbulent flows. Other well-known limitations are that 3) concentrations are computed as spatial averages in three-dimensional cells (which makes comparison with point measurements difficult and produces an

0021-8952/81/101203-09$06.25

erroneous initial dilution of those plumes whose width is smaller than the cell dimensions), and 4) relating the diffusion coefficients K to standard atmospheric measurements is difficult.

To overcome some of these limitations, some modelers have recently attempted to (i) develop new transport and diffusion techniques for the more complex applications (e.g., the particle-in-cell method; Sklarew *et al.*, 1971; Lange, 1978), or (ii) extend the applicability of the Gaussian method to such situations. In the category (ii), some extensions of Eq. (1) have been developed to treat non-stationary non-homogeneous conditions. In particular, the segmented plume approach (Chan and Tombach, 1978; Chan, 1979) and the puff approach (Lamb, 1969; Roberts *et al.*, 1970) have been successfully applied to pseudo-steady-state conditions. Both these methods break up the plume into a series of independent elements (segments or puffs) that evolve in time as a function of temporally and spatially varying meteorological conditions.

This paper will analyze the puff method and will define a new computational algorithm for the simulation of a plume by a series of puffs. The description of the basic puff method is presented in Section 2, while in Section 3 some recent improvements in the puff method are discussed and problems related to the correct application of standard puff methodology are reviewed. Section 4 contains a new puff algorithm and a method for the treatment of calm conditions, while in Section 5 the computer programming of the new methodology is briefly described. Finally, Section 6 contains a few concluding remarks concerning future applications and developments.

2. The basic puff method for plume representation

The most obvious way of treating non-stationary conditions in emissions and/or meteorology, while maintaining the Gaussian approach, is to describe the point source emission into the atmosphere by a series of "instantaneous" puffs, each one generated at every time step and containing all the mass emitted during that time interval.

Actually, real puff dispersion theory shows that puffs and plumes disperse at different rates and are governed by different theories (e.g., Pasquill, 1974). However, the representation of a plume by a series of "equivalent" (or "fictitious") puffs whose σ's evolve according to Gaussian plume theory, has been shown to be a reasonable approximation of the physical problem, which allows some degree of representation of non-stationary non-homogeneous conditions, otherwise impossible to handle with standard Gaussian theory.

If Δt is our time increment [where, in general, $\Delta t = \Delta t(t)$, a function of the time], each continuous function of the time $f(t)$ will be represented by a discrete series of values (one at each time step), where each discrete value is the average of f during the corresponding time interval. In such a way, at time t we have a discrete value $\bar{f}[t - \Delta t/2, t + \Delta t/2]$ for f, which can be considered equal to the continuous value, $f(t)$, if the function f is sufficiently "smooth" with respect to Δt.

Then, an emission rate $Q(t)$ can be represented, during the interval $[t_0 - \Delta t/2, t_0 + \Delta t/2]$, by a puff of total mass $Q(t_0)\Delta t$ generated at time t_0, with its center at the emission exit of the source. Each such puff evolves dynamically in time so that, at each time interval $[t, t + \Delta t]$ non-stationary non-homogeneous meteorological conditions (average wind and turbulence) move the center of each puff and increase the horizontal and vertical standard deviations of its concentration distribution. The concentration at each receptor is computed simply by adding the contributions of all existing puffs in the domain.

In mathematical notation, the center of a puff at time t has coordinates $\mathbf{p}(t) = [x_p(t), y_p(t), z_p(t)]$, and the average wind velocity vector at a generic point $\mathbf{p} = (x, y, z)$ during the interval $[t, t + \Delta t]$ is $\mathbf{u}(\mathbf{p}, t + \Delta t/2)$. Then the advection phenomenon can be described[1] by

$$\mathbf{p}(t + \Delta t) = \mathbf{p}(t) + \mathbf{u}(\mathbf{p}(t), t + \Delta t/2)\Delta t. \quad (2)$$

For the Gaussian steady-state general case, the plume growth is described by its horizontal and vertical standard deviations. We can assume, for example, the usual

$$\sigma_h = a_h(j_h)d^{b_h(j_h)}, \quad (3a)$$

$$\sigma_z = a_z(j_z)d^{b_z(j_z)}, \quad (3b)$$

where d is the downwind distance from the source, and a and b are empirical values, depending upon the horizontal and vertical turbulence states, j_h and j_z. Generally, the Pasquill-Gifford stability classes are used (as in Turner, 1970); they provide discrete values of $j = j_h = j_z$ for this purpose. However, many controversies exist on the definition of appropriate turbulence classification methods and sigma functions. Limitations of available methodologies and practical, useful recommendations have been defined at the AMS Workshop on Stability Classification Schemes and Sigma Curves (Hanna *et al.*, 1977).

In the puff model, each puff has its own $\sigma_h(t)$ and $\sigma_z(t)$ which grow with time. Their increase during the interval $[t, t + \Delta t]$ can be computed by know-

[1] Actually, a correct space-centered numerical method should require $\mathbf{u}\{[\mathbf{p}(t) + \mathbf{p}(t + \Delta t)]/2, t + \Delta t/2\}$ in Eq. (2). In such a case, this equation would require an iteration procedure to achieve convergence. However, in practical air pollution applications, this further refinement can be ignored. The same consideration holds for the j's turbulence states discussed below.

ing the space-time dependent turbulence states $j_h^* = j_h(\mathbf{p}(t), t + \Delta t/2)$ and $j_z^* = j_z[\mathbf{p}(t), t + \Delta t/2]$ at the center $\mathbf{p}(t)$ of the puff. This computation, however, is not straightforward, since the present "size" $\sigma_h(t)$ and $\sigma_z(t)$ of the puff depends upon the many different past diffusion conditions encountered during the entire interval $[t_0, t]$. Because of this, calculation of the growth of the sigmas during $[t, t + \Delta t]$ requires, first, the computation of a "virtual" distance, d_v (as in Ludwig *et al.*, 1977) or, more generally, virtual distances of a horizontal d_h and a vertical d_z. The virtual distance, d_h or d_z, is the downwind distance that the same puff, to have the same $\sigma_h(t)$ or $\sigma_z(t)$, would have had to travel from the source if the turbulence state had always been j_h^* or j_z^* during its entire "life" $[t_0, t]$.

In parallel with Eq. (3a), d_h is computed by

$$\sigma_h(t) = a_h^* d_h^{b_h^*}, \tag{4}$$

which gives

$$d_h = [\sigma_h(t)/a_h^*]^{1/b_h^*}, \tag{5a}$$

where $a_h^* = a_h(j_h^*)$ and $b_h^* = b_h(j_h^*)$.

Then if Δd is the downwind distance traveled by the puff in the interval $[t, t + \Delta t]$, where

$$\Delta d = |\mathbf{u}(\mathbf{p}(t), t + \Delta t/2)|\Delta t, \tag{6}$$

the new standard deviations at $t + \Delta t$ will be

$$\sigma_h(t + \Delta t) = a_h^*(d_h + \Delta d)^{b_h^*}. \tag{7a}$$

The same considerations apply to d_z, and give

$$d_z = [\sigma_z(t)/a_z^*]^{1/b_z^*}, \tag{5b}$$

$$\sigma_z(t + \Delta t) = a_z^*(d_z + \Delta d)^{b_z^*}, \tag{7b}$$

where $a_z^* = a_z(j_z^*)$ and $b_z^* = b_z(j_z^*)$.

The contribution of one puff at $\mathbf{p}(t)$ to a receptor at $\mathbf{r}$ during the interval $[t - \Delta t(t)/2, t + \Delta t(t)/2]$, for the general case of Δt time dependent, will be

$$\chi = \frac{Q(t_0)\Delta t(t_0)}{(2\pi)^{3/2}\sigma_h^2(t)\sigma_z(t)} \times \exp[-\tfrac{1}{2}|[\mathbf{p}(t) - \mathbf{r}] \div \boldsymbol{\sigma}(t)|^2], \tag{8}$$

where $\boldsymbol{\sigma}(t) = [\sigma_h(t), \sigma_h(t), \sigma_z(t)]$ and the vector notation $\boldsymbol{\gamma} = \boldsymbol{\alpha} \div \boldsymbol{\beta}$ means that its components are $(\boldsymbol{\gamma})_i = (\boldsymbol{\alpha})_i/(\boldsymbol{\beta})_i$, for $i = x, y$ and z.

In Eq. (8) note that Q and the sigmas are puff- and time-dependent, and no reflection or decay term has been considered. The concentration at $\mathbf{r}$ during the interval $[t - \Delta t/2, t + \Delta t/2]$ will be calculated by summing of contributions $\chi = \chi[\mathbf{p}(t), \mathbf{r}]$ of Eq. (8) from all existing puffs.

It must be pointed out that, if homogeneous turbulence conditions are assumed in the domain (or if turbulence states are horizontally homogeneous with no vertical wind component), the determination of the virtual distances by Eqs. (5a) and (5b) is not required at every time step, but only when there has been a change in turbulence state. However, this procedure requires the additional saving of the virtual distances of each puff at each time step.

From the preceding discussion, it is easy to recognize that, at least theoretically, this method can make a full utilization of three-dimensional time dependent meteorological inputs and, coupled with a dynamic meteorological model (or measurement interpolation technique), is capable of handling non-stationary non-homogeneous dispersion in a general complex terrain situation.

Reflection terms can be added to Eq. (8) to take into account the effects of ground and/or the inversion on each puff. In particular, Ludwig *et al.* (1977) have identified (following the suggestion of Turner, 1970) when multiple reflections should be computed and when the concentration field produced by a puff can be considered vertically homogeneous between the terrain and the inversion layer.

Finally, the total mass $Q(t_0)\Delta t(t_0)$ of each puff can be decreased at each Δt (for example, with exponential dumping terms), to taking into account 1) deposition, 2) precipitation scavenging, and 3) chemical decay.

3. Recent improvements in the puff algorithm

The puff method was improved by Sheih (1978) to take wind shear into account. Sheih's elegant algorithm describes each puff with six moving tracer particles, where the concentration distribution of each puff is determined by fitting an ellipsoid to the cluster of the six particles and assuming a three-dimensional Gaussian distribution with standard deviations equal to the half lengths of the principal axes of the ellipsoid. In this way, the departure from the standard Gaussian plume distribution increases as the plume travels further downstream due to the accumulation of the shear effect (if present in the wind data utilized by the method).

Moreover, dynamic plume rise can be considered (Sheih, 1978) where each puff is generated with some buoyancy parameters which produce, during initial several time steps, an additional vertical velocity component due to buoyancy.

The most important problem, however, in all puff models is the determination of Δt: a too large Δt produces inaccuracy in the plume description, while a too small Δt causes serious problems of computer storage and CPU running time. Ludwig *et al.* (1977) analyzed this problem and proposed a reasonable solution. In fact, it can be shown (see Fig. 1) that an infinite line string of three-dimensional equally-spaced puffs is a perfect approximation of a Gaussian plume when the separation Δd between two

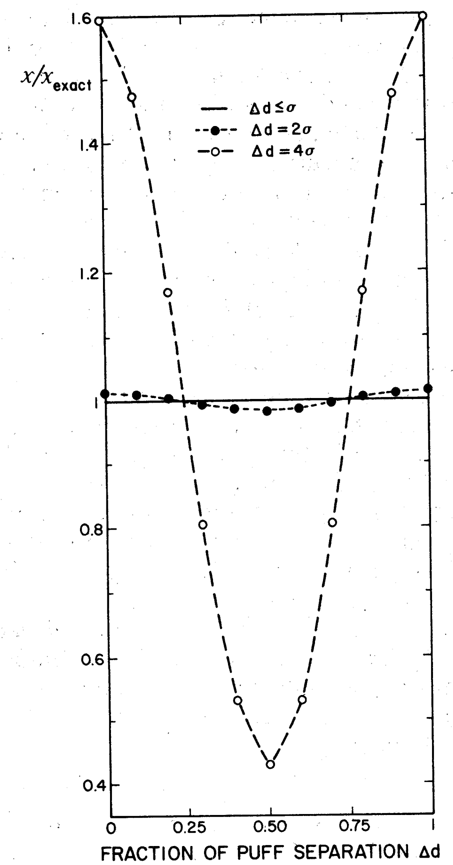

FIG. 1. Concentration χ between the centers of two puffs of an infinite string of equally-spaced puffs separated by the distance Δd (a recalculation from Ludwig *et al.*, 1977). This concentration χ is normalized by the value χ_{exact} which is obtained when Eq. (9) is met. The same behavior is found in each line parallel to the puff's centerline.

consecutive puff centers satisfies the condition

$$\Delta d \leq \sigma, \tag{9}$$

where σ is the streamwise standard deviation of the Gaussian concentration distribution of each puff.

In real non-steady cases, where we do not have infinite straight lines but, rather, segments for plume representation, Eq. (9) can still be generally used for the determination of Δt, which will be, in this way, a function of wind speed (since $\Delta d = |\mathbf{u}|\Delta t$, lower wind speed allows larger Δt). But close to the source (where σ's are very small), Eq. (9) can require a Δt of less than a few seconds, which is, for multi-source multi-hour simulations, by all means, too expensive.[2] So, Ludwig *et al.* (1977) use a reasonable Δt equal to 5 min, but at near source allow their method to generate, at each time step Δt, a sufficient number of equally spaced downwind puffs from each source to meet Eq. (9). After a while, when puffs have grown downwind, Eq. (9) is used as a criterion to allow merging puffs close together. In this way, the entire method allows a sensible reduction of the total number of puffs to be handled, still maintaining the accuracy of the computation.

Sheih (1978) minimized the above problem by incorporating the effects of mean-wind advection into the streamwise dispersion coefficient. In other words, the mean wind stretches the initial puff by $|\mathbf{u}|\Delta t$, providing reasonable overlapping between successive puffs.

However, both Ludwig's and Sheih's methods can work only in nearly steady-state conditions. In fact, if Δt is large (as the 5 min used by Ludwig *et al.*, 1977), a sudden change of wind direction can cause overestimation and/or underestimation in some receptors, as illustrated in Fig. 2 where underestimation at receptor 1 and overestimation at receptor 2 are obtained, during the interval $[t, t + \Delta t]$, even if Eq. (9) is met at each time step. Again, if we really want a fully non-stationary simulation, both puff methods can require Δt not greater than a few seconds for receptors near the sources.

It must be pointed out that Fig. 2 represents an extreme case of non-stationary conditions and that, in such a situation, the plume becomes extremely complex and requires very detailed meteorological data for its complete characterization. Therefore, the method proposed in the next section for better treating such non-stationary effects, must not be seen as the solution to the problem, but just as an improved algorithm for a more efficient simulation of the phenomenon with a reasonable amount of meteorological input data.

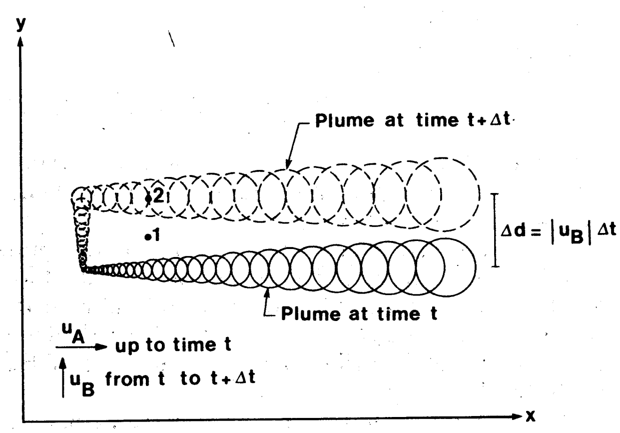

FIG. 2. Calculated positions of puffs after a sudden change in wind direction. The circles indicate one standard deviation from the center of each puff.

[2] It must be remembered that the puff method is just a representation of the plume by a series of independent equivalent puffs. Even with very small Δt, the nature of the whole problem remains the plume dispersion simulation over time averages sufficiently large to avoid short-term variations (e.g., the horizontal wind meander).

4. The AVPPM[3] puff method

a. Puffs handling

The method the author has developed handles general non-stationary conditions without creating serious computer storage and CPU time-consumption problems, since Δt, the time increment chosen, is sufficiently large (e.g., 5–10 min). All the mass emitted in the interval $[t_0, t_0 + \Delta t]$ is concentrated in the puff generated at t_0. Since such puffs do not meet the condition required by Eq. (9), we can say that a string of consecutive puffs from the same source gives only the geometry of the plume evolution, where a "segment" of the plume is represented by the area between two consecutive puffs. However, the puff masses cannot be directly used for computation of the contribution at the receptors since Eq. (9) is not met (see Fig. 3).

At each time step (say, $t + \Delta t$), all information about the status of the present puffs (at time $t + \Delta t$) and previous puffs (at time t) must be available and an array "chain" is used for relating each puff to its original source according to its age.

If a given source has generated n puffs in the domain at time t (and, therefore, $n + 1$ puffs at time $t + \Delta t$), it can be seen from Fig. 3 that n three-dimensional quadrilaterals can be defined, where the vertices of each quadrilateral are determined by the positions of two consecutive puffs at time *t and* $t + \Delta t$. In particular, Fig. 3 shows that all mass emitted from S and located at time t in the segment AB is concentrated in A, which moves to A′ in the time interval $[t, t + \Delta t]$. Actually, this mass has affected the quadrilateral ABB′A′ during the interval $[t, t + \Delta t]$. The quadrilaterals need not lay on a plane and may be degenerate. Each of the n quadrilaterals must be analyzed for the computation of its contribution to each receptor, and the entire method must be repeated for all sources at every time step.

[3] AeroVironment puff plume model.

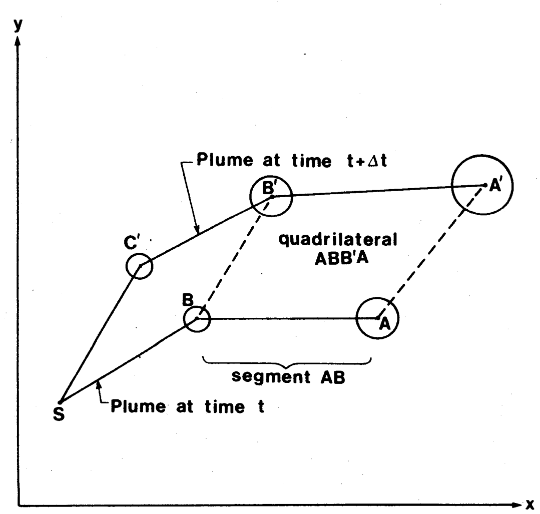

FIG. 3. Schematic diagram showing the method by which emitted mass distribution is treated. The circles have the same meaning as in Fig. 2.

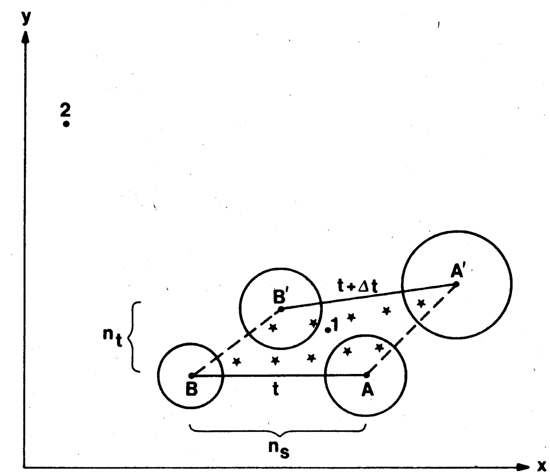

FIG. 4. Analysis of one quadrilateral (the circles have the same meaning as Fig. 2). The contribution to receptor 2 is zero while, for computation at receptor 1, $n_t \times n_s$ puffs are generated (splitting technique with σ's interpolation) in the quadrilateral ABB′A′ and are indicated by asterisks ($n_s = 5$, $n_t = 2$).

This computation (see Fig. 4) first requires an analysis to see if the quadrilateral gives a nonzero contribution at a receptor. To this end, the closest point in the quadrilateral to the receptor is found. If the distance of this point from the receptor is more than, say 4 or 5 σ's, the contribution is zero (as in receptor 2). Otherwise, the mass of the puff at A, which has been moved to A' (but could have lost mass due to deposition or chemical decay), must be redistributed in the quadrilateral according to the real physics of the non-stationary dispersion. To this end, a splitting technique is applied to the quadrilateral, with an artificial generation of a sufficient number of puffs in its area so that Eq. (9) is met. This can be done, for example, as illustrated in Fig. 4 (using the more critical upwind puffs which have smaller σ's), where the number n_s can be computed by applying Eq. (9) to the "old" segment AB, while n_t can be computed by applying Eq. (9) to the "upwind" segment BB′ or better, to its component normal to AB. The characteristics of each new puff (center position and σ's) are obtained by interpolation among the known characteristics of the four puffs, A, B, B′, A′.

The first downwind quadrilateral contains the source. Some information on initial spread of the plume (e.g., as a function of the plume rise or of the exit diameter of the source) can be used for supplying σ values at the source point to allow the interpolation computation in this first quadrilateral.

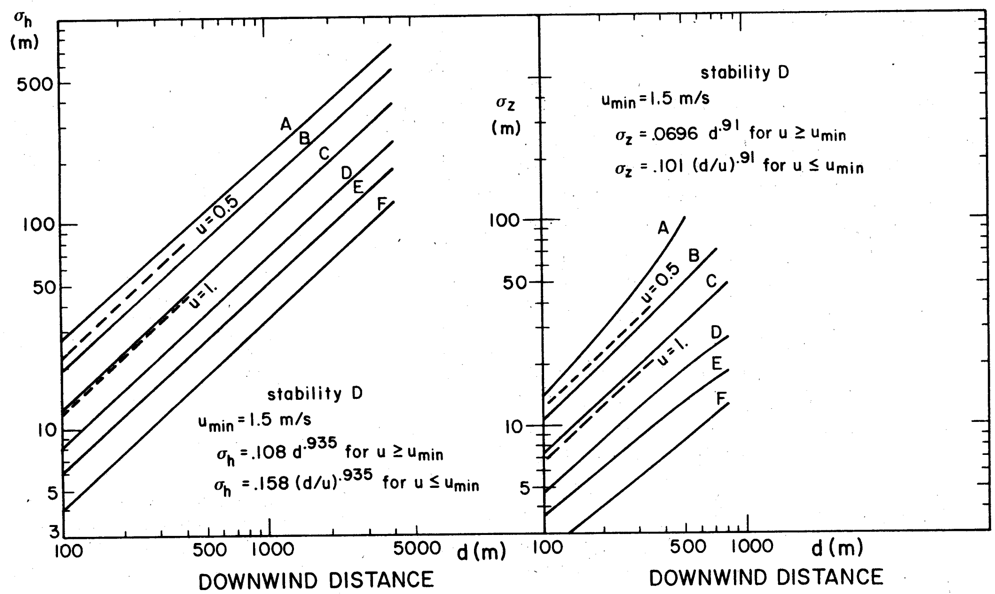

FIG. 5. An example of calm conditions treatment in the puff method. Solid lines are the common σ functions (source: Turner, 1970), while dashed lines represent the downwind growth of a puff in neutral D stability when $u < u_{\min}$.

It must be noted that this splitting technique will be applied only when required for a particular receptor. In this way, we solve our computer storage and time problems without losing the accuracy of the computation.

b. The calm situations

This problem can be solved by allowing Eqs. (3a) and (3b) to work as a function of time (more exactly, the age) instead of downwind distance. In fact, if $t - t_0$ is the age of the puff, the formula

$$\sigma = ad^b \tag{10}$$

is equivalent in some way to

$$\sigma = a[u(t - t_0)]^b = au^b(t - t_0)^b = a'(t - t_0)^b, \tag{11}$$

where u is the average wind speed, and $a' = au^b$.

For wind speed less than a fixed value $u_{\min}$ (e.g., the instrument minimum significant value), a' can be kept fixed to the value $a'_{\min}$, where

$$a'_{\min} = au^b_{\min}, \tag{12}$$

which allows Eq. (11) to work for calm conditions as a function of the age of the puff. In other words, we can say that if Eq. (10) holds for transport conditions ($u \geqslant u_{\min}$), and

$$\sigma = a'(t - t_0)^{b'} \tag{13}$$

holds for calm situations ($u \leqslant u_{\min}$), then Eq. (11) in the case $u = u_{\min}$ requires both $a' = a'_{\min}$, and $b' = b$.

In the puff method, for the sigmas growth computation between t and $t + \Delta t$, the concept of virtual distance can be extended to that of horizontal and vertical virtual ages, t_h and t_z. They are computed in a way similar to that in Section 2. We obtain relations similar to Eqs. (5a) and (5b), i.e.,

$$t_h = [\sigma_h(t)/a_h^{**}]^{1/b_h^{**}}, \tag{14a}$$

$$t_z = [\sigma_z(t)/a_z^{**}]^{1/b_z^{**}}, \tag{14b}$$

where $a_h^{**} = a_h^* u_{\min}^{b_h^*}$, $b_h^{**} = b_h^*$, $a_z^{**} = a_z^* u_{\min}^{b_z^*}$, $b_z^{**} = b_z^*$, and a_h^*, b_h^*, a_z^* and b_z^* have been defined in Section 2.

The virtual age t_h or t_z is the age that the same puff, to have the same $\sigma_h(t)$ or $\sigma_z(t)$, would have had if the turbulence state had always been $j_h^* = j_h[\mathbf{p}(t), t + \Delta t/2]$ or $j_z^* = j_z[\mathbf{p}(t), t + \Delta t/2]$ during $[t_0, t]$.

In such a calm situation case, Eqs. (7a) and (7b) can be rewritten as

$$\sigma_h(t + \Delta t) = a_h^{**}(t_h + \Delta t)^{b_h^{**}}, \tag{15a}$$

$$\sigma_z(t + \Delta t) = a_z^{**}(t_z + \Delta t)^{b_z^{**}}, \tag{15b}$$

The above method, after the determination of $u_{\min}$, gives a consistent way of treating the growth of σ_h and σ_z when calm conditions are found in the interval $[t, t + \Delta t]$. However, experimental data are expected to give a better estimate of a^{**} and b^{**} and to validate the entire procedure.

Fig. 5 shows the behavior of σ_h and σ_z, according to the above proposed methodology, when $u < u_{\min}$.

c. Use of more complex σ formulas.

Often, particular situations—for example, dispersion in complex terrain—have been better simulated by σ formulas different from Eq. (10), as in the case shown by Mullen *et al.* (1977), where equations like

$$\sigma = p + qd^r(1 + 3 \times 10^{-4}\, d)^s \qquad (16)$$

are proposed (p, q, r, s are empirical parameters which are a function of atmospheric turbulence, terrain roughness, and meteorological measurements). If formulas of this type must be used, the determination of the virtual distances or ages is not straightforward as in Eqs. (5a) and (5b) or (14a) and (14b), and an iterative algorithm (e.g., the Newton-Raphson's method) may be required.

d. Segment, area and volume sources

The proposed method can be easily extended to segment, area and volume sources. They can be represented, respectively, by the evolution of 2, 4 and 8 puffs in the domain, where, in the interval $[t, t + \Delta t]$, an analogous splitting method using considerations similar to those developed in the quadrilateral of Fig. 4 are applied. In this case, the emission due to the entire segment (or area or volume source) is concentrated into 2 (or 4 or 8) tracing puffs and when required by the receptor position these masses must be spread into volume elements (now the "vertices" of the quadrilaterals consist of 2, 4 or 8 tracing puffs) to satisfy both Eq. (9) and to maintain the accuracy of the non-stationary computation. However, we think that only the segment sources, perhaps, will require such a refined methodology, while area and volume sources should be better treated by grid models.

e. Other improvements

Special dispersion conditions have given experimental data for which a better fit could be obtained if a different diffusion were allowed 1) crosswind and downwind (e.g., complex terrain situations), and 2) above and below the centerline of the puffs (e.g., vertical stratification effects). As an empirical improvement, these effects can be taken into account by describing the size of the puff with four σ's: σ_x, σ_y, σ_z^+, σ_z^-, where σ_z^+ is the standard deviation above, and σ_z^- below the puff center. In particular, the evolution of the two σ_z's will take into account the average stability in the area (growing with time) affected by the puff (e.g., one σ_z^+ in the vertical above, and one σ_z^- below).

Reflection on the ground can be computed by adding the contribution of an imaginary equivalent puff at $[x_p, y_p, \bar{z}_g - (z_p - \bar{z}_g)]$, where

$$\bar{z}_g = \tfrac{1}{2}[z_g(x_p, y_p) + z_g(x_r, y_r)] \qquad (17)$$

is the mean elevation on the ground between that of the puff, $z_g(x_p, y_p)$, and that of the receptor, $z_g(x_r, y_r)$; naturally, all z's must be computed with respect to the same reference level, e.g., sea level. The contribution of this imaginary puff will be multiplied by a reflection coefficient (between 0 and 1). This same reflection technique can also be applied to the inversion layer.

When a puff is sufficiently large, its evolution can probably be better described by a grid model. For example, when the σ's are of the size of the grid cell, the puff can be erased together with a corresponding mass generation in the coupled grid model for handling of long-range effects. The puff method alone, therefore, is seen to work better for short-range near-field simulations.

f. Puff model comparison with the steady-state Gaussian formula

A complete validation of the model will be performed when tracer data in non-stationary conditions are available. However, the first operative FORTRAN-language version of the puff method (AVPPM/2A), which incorporates the concepts described previously, has been successfully tested against the Gaussian steady-state formula of Eq. (1). A case like that described in Fig. 6, which should require Δt of the order of 10 s with the basic puff method, can be accurately treated with Δt of one order of magnitude greater. In fact, in Fig. 6, Δd is one order of magnitude greater than σ values above most of the receptors.

However, simulation runs have pointed out the importance of using an accurate splitting technique. In fact, if the σ's values (of the artificial puffs generated in the quadrilateral) are calculated by a simple linear interpolation between existing puffs, we introduce a numerical error since the real σ's evolution is not linear but is described, for example, by Eq. (10). In the case of Fig. 6 (with $b = 0.78 < 1$), the linear interpolation produces a systematic underestimation of the σ's of the interpolated puffs, which causes concentration underestimation before the maximum downwind ground-level concentration and overestimation after. Naturally, the opposite effect has been obtained with $b > 1$.

Fig. 6 shows how the above numerical approximation (linear σ's interpolation in the splitting method) requires, in that particular case, a Δt less than, say, 3 min in order to maintain some good computational accuracy. However, a large Δt can be used if a more realistic interpolation is used. For example, in the artificial puff generation technique shown in Fig. 4, Eq. (10) can be used for the determination of the σ's of the puffs inside the quadrilateral.

Numerical tests using the correct exponential interpolation of Eq. (10) have shown that this more

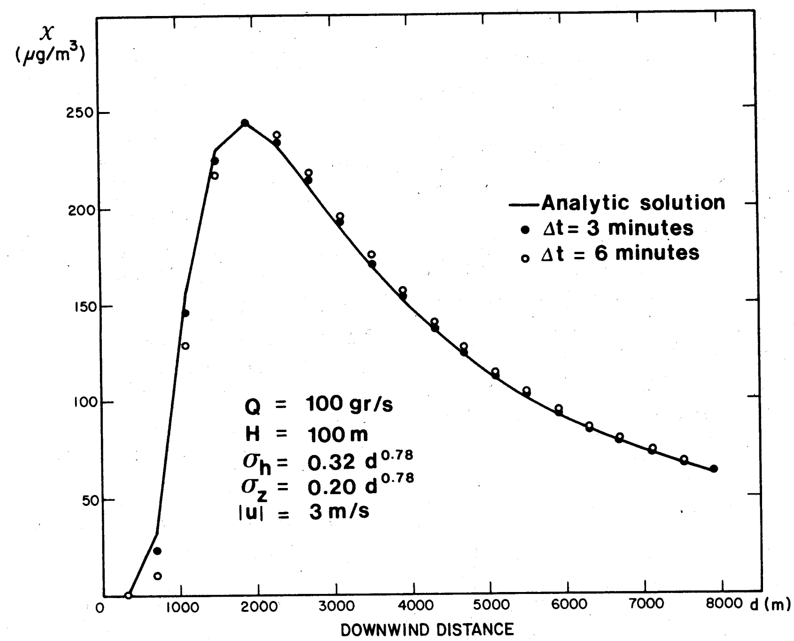

FIG. 6. Comparison of the AVPPM method (with σ's linear interpolation) with the steady-state Gaussian formula of Eq. (1). Concentration χ is computed at ground-level receptors downwind to the source (crosswind distance, $c = 0$).

accurate computation is particularly important for splitting inside the first quadrilateral (the one which contains the source), where the linear interpolation produces its highest error. However, the linear interpolation is computationally faster and, with some attention to the determination of the Δt values as a function of wind speed and receptor locations, can give satisfactory results.

5. The programming code

The code (AVPPM/2A) handles multiple point sources and multiple receptors and requires topographical, meteorological and emission input information in general complex terrain. Essentially, the puff dispersion code utilizes a "chain" vector for relating all puffs at t and $t + \Delta t$ generated by each source. This chain gives the index numbers of all required puffs so allowing the computation of each source contribution in each receptor. The generation of a new puff is done by creating a new entry in the next free area of the main puff storage array and by adding the entry index to the chain. The erasing of out-of-boundary puffs is done by shifting the indices in the chain (the newest puffs are at the end of the chain of each source) and by setting free-area switches in the main puff storage array.

At each interval $[t, t + \Delta t]$, both old (t) and new ($t + \Delta t$) puff parameters are available and the computation, according to the above methodology, can then proceed to the next time step, when new puffs become old and a newer configuration is computed.

Finally, the splitting algorithm does not require a special storage for the additional puffs generated, since a loop can be defined for the accumulation of different contributions due to the imaginary puffs interpolated in the quadrilateral area.

6. Conclusions

A new puff dispersion algorithm for plume representation has been discussed. The methodology, reasonable in computer storage and CPU time, allows a fairly good representation of the air pollution dispersion even in the most accentuated non-stationary non-homogeneous meteorological and emission conditions. The method should improve our air pollution simulation capabilities, especially for short-term, short-range simulations, and where high quality meteorological data are available (e.g., Doppler acoustic sounder measurements). In particular, this method should work better with both a meteorological input model (for supplying a three-dimensional meteorological field), and a grid model (for the downwind long-range evolution of the puffs).

Experimental data are expected to validate this approach, especially the algorithm which allows the treatment of calm conditions. Data are also expected to suggest puff concentration distributions different from the Gaussian one. These new distributions, in fact, could be easily incorporated in the proposed method.

Acknowledgments. The author is grateful to Dr. I. H. Tombach and Mr. A. L. Davis of AeroVironment Inc. for their technical review of the manuscript. Appreciation is extended to Drs. F. L. Ludwig (SRI International) and C. M. Sheih (Argonne National Laboratory) for their useful suggestions. This study has been partially supported by the Western Oil & Gas Association (WOGA).

REFERENCES

Chan, M. W., 1979: A tracer experiment to determine the transport and diffusion of an elevated plume in complex terrain. 72nd Annual Meeting of the APCA, June 24–29, Cincinnati, OH [Available from the author].

——, and I. H. Tombach, 1978: AVACTA—Air pollution model for complex terrain applications. AeroVironment Inc., Pasadena, CA, Rep. AV-M-8213. [Available from the author].

Hanna, S. R., G. A. Briggs, J. Deardorff, B. A. Egan, F. A. Clifford and F. Pasquill, 1977: AMS workshop on stability classification schemes and sigma curves—summary recommendations. *Bull. Amer. Meteor. Soc.*, **58**, 1305–1309.

Lamb, R. G., 1969: An air pollution model of Los Angeles. M.S. thesis, University of California, Los Angeles, 120 pp [see Lamb, R. G., and M. Neiburger, 1971: An interim version of a generalized urban diffusion model. *Atmos. Environ.*, **5**, 239–264].

Lange, R., 1978: ADPIC—A three-dimensional particle-in-cell model for the dispersal of atmospheric pollutants and its comparison to regional tracer studies. *J. Appl. Meteor.*, **17**, 320–329.

Lugwig, F. L., L. S. Gasiorek and R. E. Ruff, 1977: Simplification of a Gaussian puff model for real-time minicomputer use. *Atmos. Environ.*, **11**, 431–436.

Martin, D. O., 1971: An urban diffusion model for estimating long-term average values of air quality. *J. Air Pollut. Control Assoc.*, **21**, 16–23.

Melli, P., and E. Runca, 1979: Gaussian plume model parameters for ground-level and elevated sources derived from the atmospheric diffusion equation in a neutral case. *J. Appl. Meteor.*, **18**, 1216–1221.

Mullen, J. B., M. W. Chan and I. H. Tombach, 1977: Development and validation of a model for diffusion in complex terrain. *Preprints Joint Conference on Applications on Air Pollution Meteorology*, Salt Lake City, Amer. Meteor. Soc., 188–191.

Pasquill, F., 1974: *Atmospheric Diffusion*. Ellis Horwood Limited, 429 pp.

Roberts, J. J., E. S. Croke and A. S. Kennedy, 1970: An urban atmospheric dispersion model. *Symposium on Multiple-Source Urban Diffusion Models*. Air Pollut. Control Office Publ. No. AP-86, pp. 6.1–6.72 [Available from the author].

Runca, E., P. Melli and P. Zannetti, 1976: Computation of long-term average SO_2 concentration in the Venetian area. *Appl. Math. Model.*, **1**, 9–15.

Sheih, C. M., 1978: A puff pollutant dispersion model with wind shear and dynamic plume rise. *Atmos. Environ.*, **12**, 1933–1938.

Sklarew, R. C., A. J. Fabrik and J. E. Prager, 1971: A particle-in-cell method for numerical solution of the atmospheric diffusion equation, and application to air pollution problems. Systems, Science and Software, La Jolla, CA, Rep. 3SR-844 [NTIS PB 209–290].

Turner, D. B., 1970: Workbook for Atmospheric Diffusion Estimates. EPA Rep. AP-26 [NTIS PB 191–482].

U.S. Environmental Protection Agency, 1978: Guideline on Air Quality Models. EPA-450/2-78-025, OAQPS No. 1.2-080 [NTIS PB 288–783].